Applying Dual-Sensor Streamer Technology to a Guyana 2-D Survey

Jack Kinkead, Lorin Friedberg Cramer, Quoi Truong, Dave Carlson, PGS

This paper was prepared for presentation during the 11th International Congress of the Brazilian Geophysical Society held in Salvador, Brazil, August 24-28, 2009.

Abstract

Dual-sensor technology allows one to separate the up-going and down-going wave fields, and ultimately remove the receiver ghost. This increases the spectral bandwidth of the recorded data and results in a final image that is improved for all depths. Application of this technology in offshore Guyana has resulted in an improved image of the subsurface as compared to what could be achieved with more conventional streamer technology.

Introduction

The concept of using two sensors to eliminate the ghost associated with the water surface was first proposed over 60 years ago. Until recently, the only practical implementation of this idea was in the form of cables and other devices deployed along the ocean bottom or in some other stationary arrangement.

In 1989, Barr and Sanders presented work on how to effectively utilize collocated pressure and velocity detectors within a water bottom cable. They showed that this arrangement was superior to other methods at that time, although it still required knowledge of the seafloor reflection coefficient to obtain the correct upgoing wave field solution.

In the last few years, the issues of deploying a velocity sensor with its companion pressure sensor within a towed streamer have been overcome. In 2007, Carlson et.al. and Tenghamm et.al. presented their work on the dual-sensor streamer technology demonstrating how it could be used to combine the benefits of dual-sensor with the efficiency of a towed streamer.

In this paper we will summarize the theory of using dual sensors to eliminate the receiver ghost. We will then cover in more detail the acquisition and processing which was performed. We will finish with comparisons of an "upgoing pressure" product and the corresponding (traditional) hydrophone only result along with our conclusions.

Dual Sensor Theory

In figure 1, the wavelets associated with a pressure and velocity sensors within a cable are depicted in blue and red respectively.

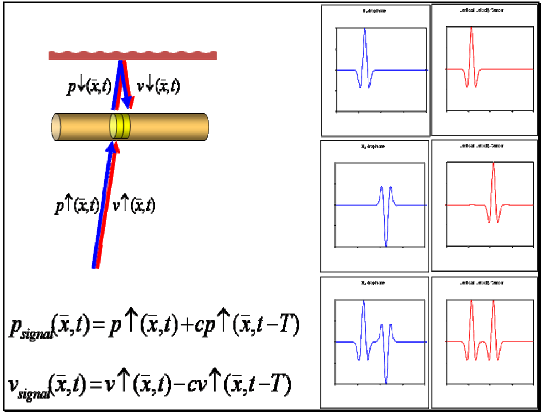

Figure 1.

Note that the initial response from the upward moving wave field has the same polarity for both sensors, however the downgoing surface reflection (also known as a surface ghost response) has resulted in responses with opposite polarity. By correctly summing these two responses from the different sensors, one can effectively eliminate the surface ghost.

Guyana 2D survey

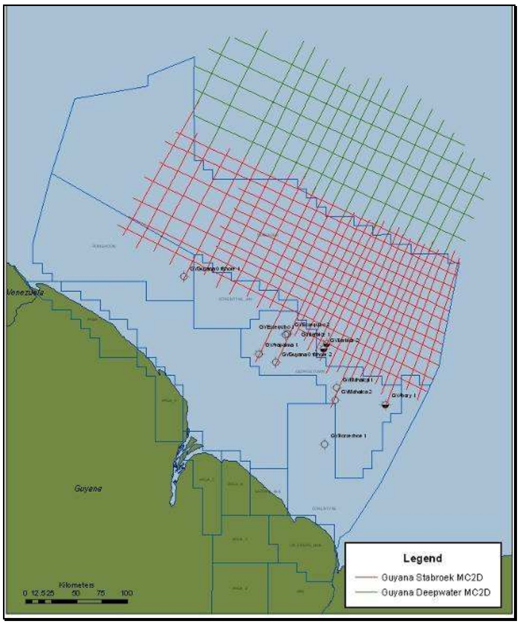

Figure 2.

The survey (see fig 2) comprises 11,500 kilometers of 2D seismic arranged in an orthogonal grid pattern covering an area of approx 90000 square kilometers. The area was shot in two phases. Our data examples will be culled from the Phase I area (in red) which is nearer the shore.

A single source vessel towing a dual sensor cable 12 kilometers in length was used. Along the length of the cable are collocated arrays of hydrophones and velocity sensors, comprising a total of 1920 individual channels towed at a depth of 15 meters. The source array consisted of 6 subarrays towed at a 9 meter depth, comprising a total volume of 8260 cu.in. and actuated with a pressure of 2000 psi. The full array was fired at a 37.5 meter interval and recordings made of the subsequent 14.3 seconds.

Data Processing

Data processing consisted of the following sequence of steps:

- Noise removal
- Wave field separation
- Tau – p Demultiple
- Surface Related Multiple Elimination (SRME)
- Hi-Resolution Radon
- Q compensation
- Pre-Stack Time Migration

Noise Removal

Prior to wave field separation, it is necessary to remove noise which may degrade the process. Two major types of noise encountered were bird noise and cable strum.

The bird noise was associated with the physical devices attached to the cable to maintain a desired depth. This noise type was more prevalent on the velocity sensor data due to the induced vertical motion.

The cable strum is caused by a tugging on the cable, by the tail buoy assembly. This noise type was more prevalent on the hydrophone data due to its primarily horizontal motion.

The bird noise was addressed with an f-x based technique. This technique utilizes iterative f-x prediction error filtering of the noisy data coupled with a back-substitution of the signal. This process is performed over discrete time and spatial windows.

Figure 3 shows a comparison of the velocity sensor shot records before and after the noise attenuation. Note the dramatic reduction in the noise level, allowing the underlying signal events to emerge.

The cable strum was addressed with a Fourier model based approach. The noise was modeled from the raw data using a pass region encompassing the noise. This was then subtracted from the raw record.

Velocity sensor
Before / After noise attenuation

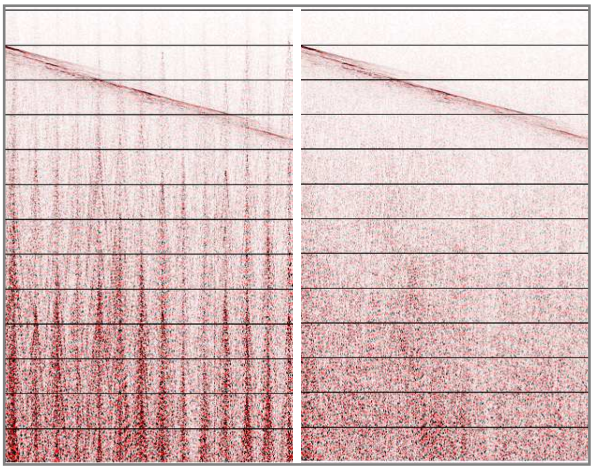

Figure 3

Hydrophone
Before / After noise attenuation

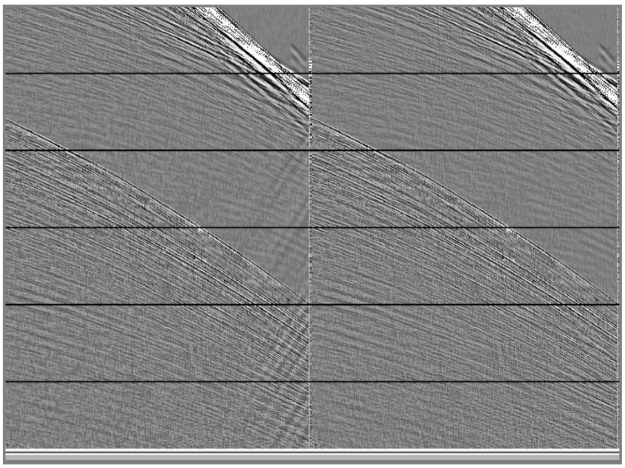

Figure 4.

Figure 4 shows the hydrophone shot record before and after the noise attenuation. Note how well the linear noise is removed from the right side of the record.

Wave field Separation

This process takes the two wavefields recorded from the hydrophone and velocity sensor to generate the upgoing pressure field.

Figure 5, compares the spectra from the two sensor types and the upgoing pressure field derived from them. These spectra have been measured directly from the recorded shots.

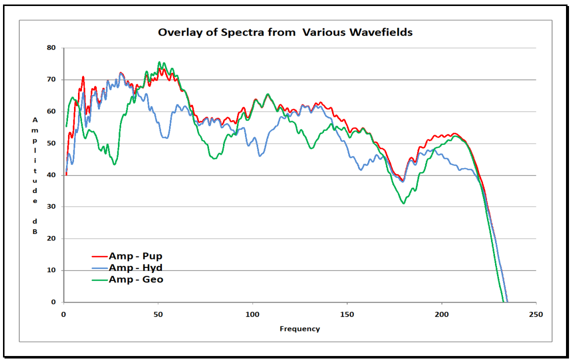

Figure 5.

The hydrophone and velocity sensor are shown in blue and green respectively. The spectral notches are evident on both of these sensors and are aligned such that a notch from one sensor type aligns with a peak in the spectra from the other sensor type.

When the hydrophone and velocity sensor are processed to obtain the upgoing pressure, shown in red, the resultant spectrum is void of the notches. The remaining notches centered around 85 and 170 Hz are due to the Source ghost.

Demultiple method

The survey area exhibits a large change in the water depth. In order to accommodate this large variation, a combination of tau-p decon, SRME, and Hi-Resolution Radon were used.

Before / After tau-p and SRME "Shallow Water"

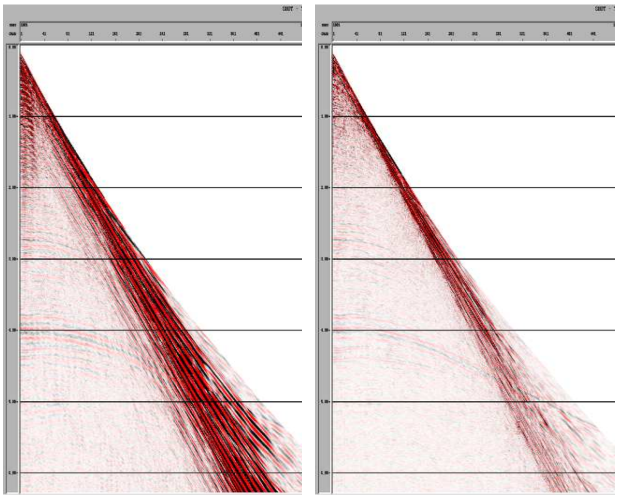

Figure 6.

The tau-p decon and SRME were combined in a hybrid approach which allowed the tau-p decon to attack the near surface multiple generating layers, followed by the SRME to finish the task of removing any remaining surface multiple energy.

As the water depth increased, the tau-p decon was ramped off, and the SRME was allowed to work on the full seismic section.

Figure 6 shows the results after applying the tau-p decon in the shallower water. In addition to removing the reverberation, the application of mutes in the transform domain allows the attenuation of additional noise.

Figure 7 shows the result after application of SRME on a deep water shot. Note how the multiple with its broader spectrum is attenuated effectively by the demultiple application.

Before / After SRME "Deep Water"

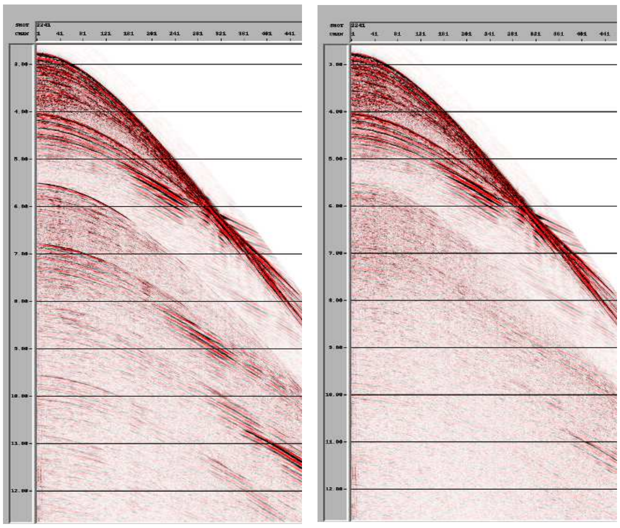

Figure 7.

Before / After Hi-Res radon

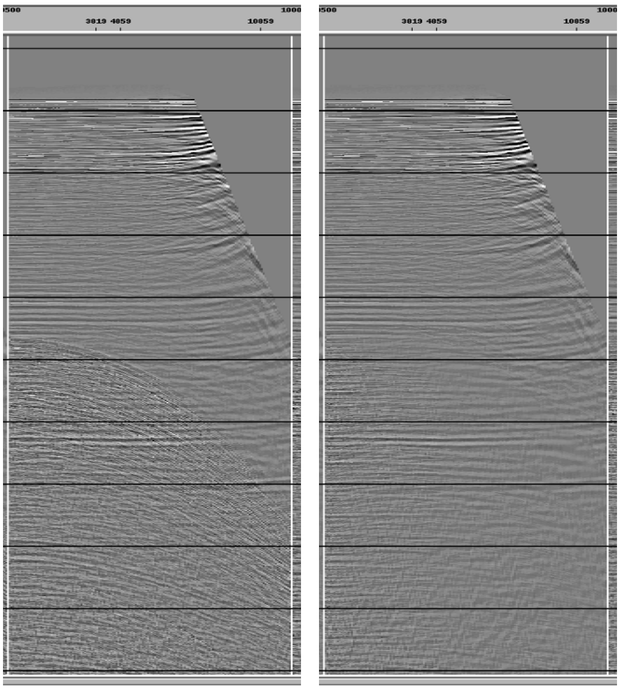

Figure 8.

Figure 8 shows the result after applying a high resolution radon demultiple process to a CMP gather.

Compensating for Q attenuation

Q attenuation is the phenomena associated with the earth's response to a propagating wavefield. As the wavefield propagates it experiences a frequency dependent decay in amplitude, and a dispersion of the wavefield caused by the frequency dependent velocity of the subsurface.

Various methods can be utilized to estimate the Q value associated with the seismic wavefield. The methods which rely on the use of estimating Q from the spectral decay benefits from the broader bandwidth achieved with the dual-sensor streamer. Without the notches, the resultant spectra are more easily analyzed to determine a rate of decay in amplitude for individual frequency components. These statistics can then be converted into effective Q values.

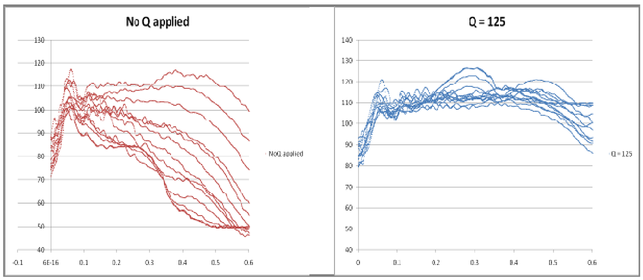

Figure 9.

In figure 9, the spectra obtained from a series of time gates are shown. The gates were placed at increasing time depth to observe how the spectra changes as a function of depth in the subsurface.

The spectra on the left are from a pstm stack, where Q compensation has not been applied. Note the wide fan shape of the spectra.

The spectra on the right are after the application of Q compensation. Note how the spectra effectively overlap one another indicating this value of Q is doing an adequate job of removing the earth's Q effect.

Examples of Stacks

The displays which follow show comparison stacks of the upgoing pressure wavefield against the hydrophone only recording. In the first comparison we show an area from an intermediate water depth. The improved resolution of the various boundaries is a consequence of the improved bandwidth achieved with the dual-sensor streamer. The next comparison is from an area where the water depth is greater, and shows the improvement in image quality from the water bottom to the deeper section.

Conclusions

The project has been extremely successful. Its initial objectives were to obtain superior imaging of the subsurface, especially in the deep section. The upgoing pressure result has achieved a very broad bandwidth result, and has resulted in images superior to that achievable with a conventional streamer.

Acquisition went smoothly and the hardware performed flawlessly for the full length of the survey.

The processing of the data has gone very smoothly as well, with delivery of the two phases occurring on schedule.

Acknowledgments

The authors wish to thank PGS for permission to publish this work. Also a special thanks to our coworkers for their invaluable assistance and support

References

Barr, F.J. and Sanders, J.I. [1989] Attenuation of water-column reverberations using pressure and velocity detectors in water-bottom cable. *Annual Meeting Expanded Abstracts*, SEG, 653-656.

Carlson, D., Söllner, W., Tabti, H., Brox, E., and Widmaier, M. [2007] Increased resolution of seismic data from a dual-sensor streamer cable. *Annual Meeting Expanded Abstracts*, SEG, 994-998.

Tenghamn, R., Vaage, S., and Borresen, C. [2007] A dual-sensor, towed marine streamer; its viable implementation and initial results. *Annual Meeting Expanded Abstracts*, SEG, 989-993.

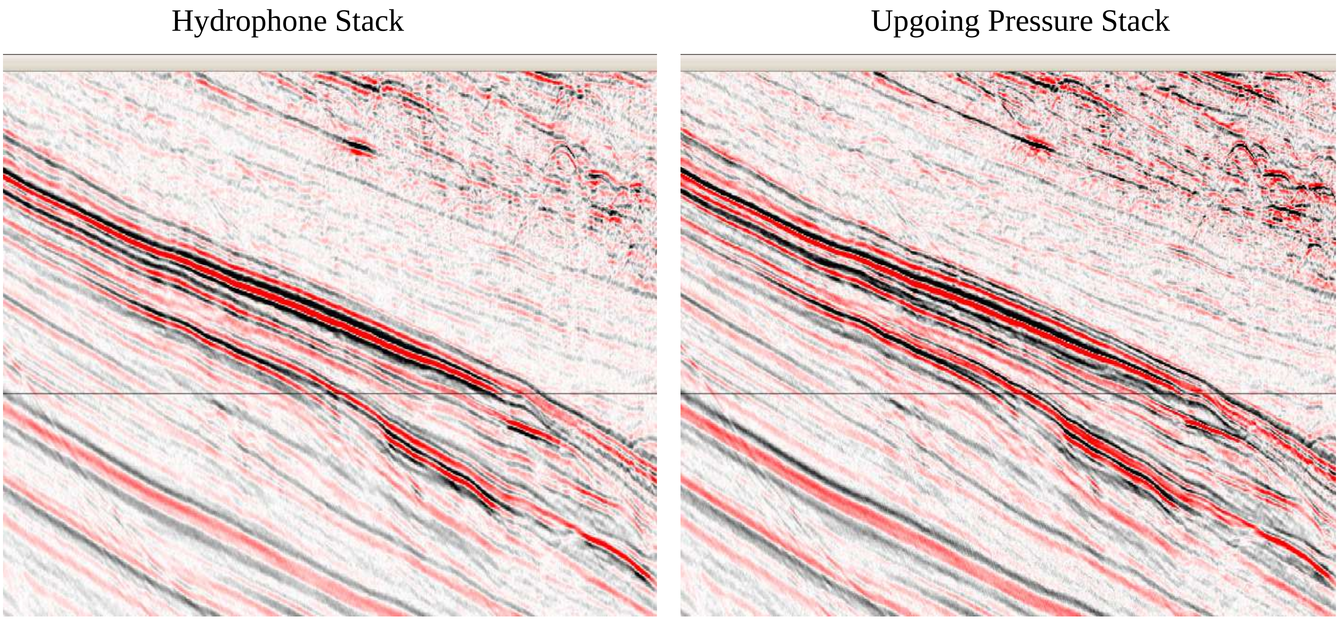

Hydrophone Stack

Upgoing Pressure Stack

These stack displays were taken from an area in Phase I where the water bottom slopes from 1.0 to 1.8 seconds. The image is a window centered around 3.0 seconds.

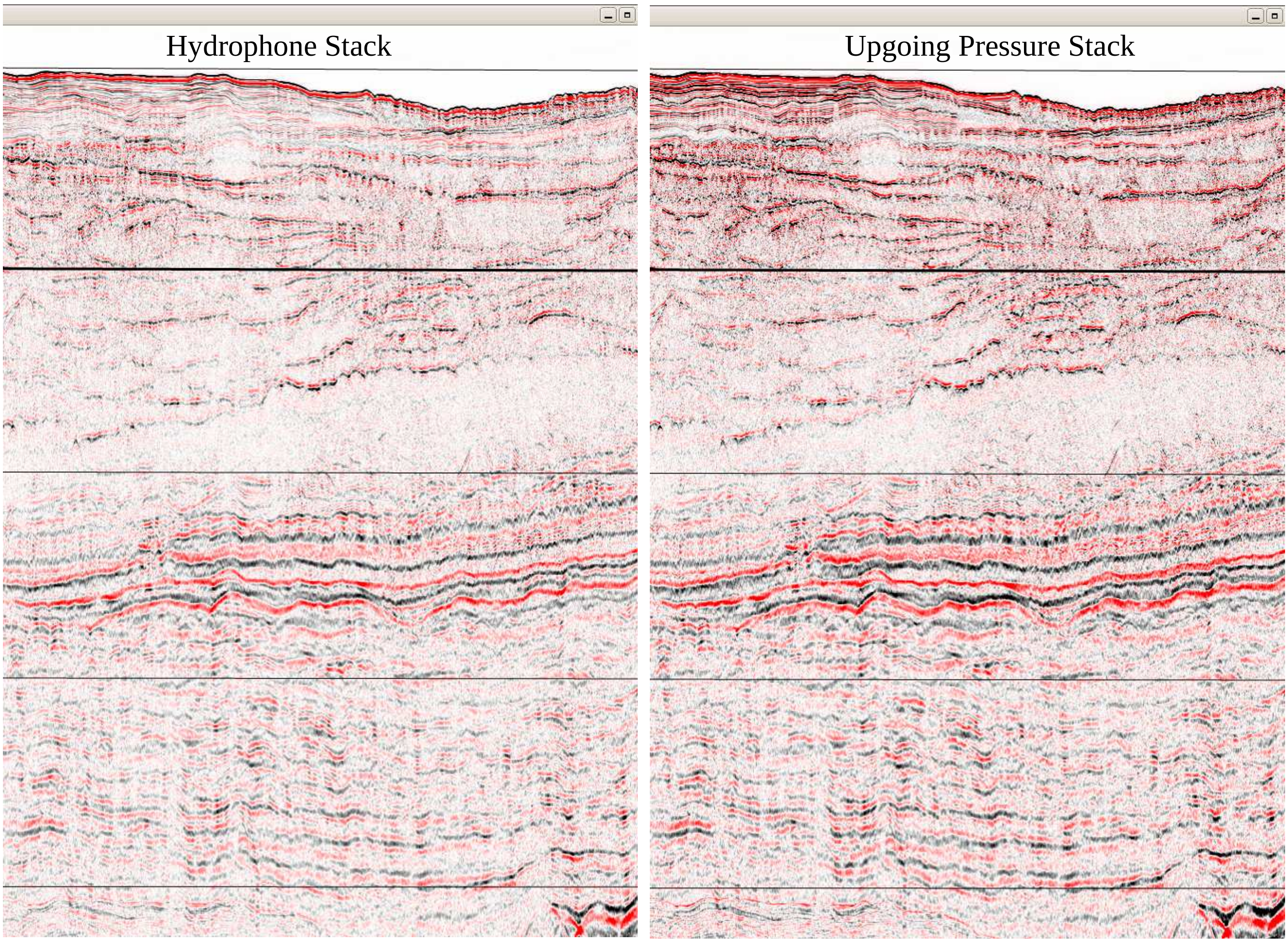

Hydrophone Stack

Upgoing Pressure Stack

These displays were taken from an area in Phase I where the water bottom is near its maximum of 4.0 seconds. The image shows the image from 4.0 to 8.3 seconds.